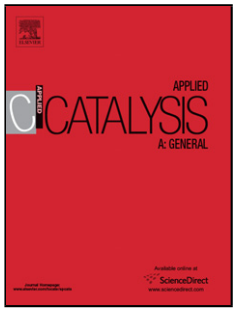

Title: Propane ammoxidation on Bi promoted $MoVTeNbO_x$ oxide catalysts: Effect of reaction mixture composition

Author: Tamara V. Andrushkevich Galina Y. Popova Yuriy A. Chesalov Evgeniya V. Ischenko Mikhail I. Khramov Vasily V. Kaichev

PII: S0926-860X(15)30129-0
DOI: http://dx.doi.org/doi:10.1016/j.apcata.2015.08.034
Reference: APCATA 15528

To appear in: *Applied Catalysis A: General*

Received date: 27-5-2015
Revised date: 31-7-2015
Accepted date: 27-8-2015

Please cite this article as: Tamara V.Andrushkevich, Galina Y.Popova, Yuriy A.Chesalov, Evgeniya V.Ischenko, Mikhail I.Khramov, Vasily V.Kaichev, Propane ammoxidation on Bi promoted MoVTeNbOx oxide catalysts: Effect of reaction mixture composition, Applied Catalysis A, General http://dx.doi.org/10.1016/j.apcata.2015.08.034

Propane ammoxidation on Bi promoted $MoVTeNbO_x$ oxide catalysts: Effect of reaction mixture composition

Tamara V. Andrushkevich[a*] andrushk@catalysis.ru, Galina Y. Popova[a], Yuriy A. Chesalov[a,b], Evgeniya V. Ischenko[a,b], Mikhail I. Khramov[c], Vasily V. Kaichev[a,b]

[a]Boreskov Institute of Catalysis SB RAS, Lavrentieva str, 5, Novosibirsk, 630090, Russia

[b]Novosibirsk State University, Pirogova str., 2, Novosibirsk, 630090, Russia

[c]Ascend Performance Materials LLC., P.O. Box 97, Gonzalez, FL 32560-0097, USA

[*]Corresponding author. fax +7 383-3308056.

Graphical Abstract

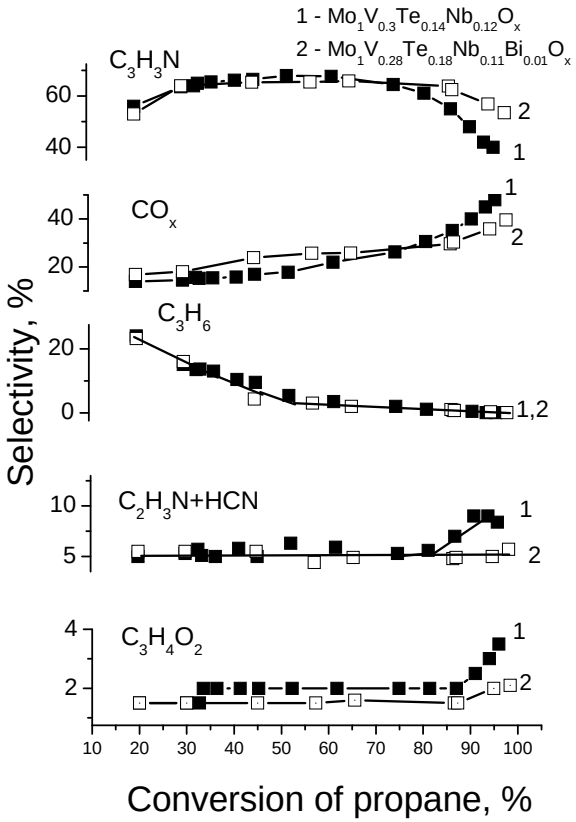

Highlights

►MoVTeNb catalyst promoted by Bi was studied in propane ammoxidation.

►Bi-modified MoVTeNb catalyst demonstrates increased selectivity to acrylonitrile.

►The transformation of acrylonitrile is lowered due to decreased catalyst acidity.

►The effect of propane, ammonia, and oxygen concentrations was investigated.

ABSTRACT

MoVTeNbO catalysts were characterized with XRD, XPS, and FTIR techniques and tested in the ammoxidation of propane. Bismuth-modified MoVTeNbO catalysts showed a higher acrylonitrile yield than the base four-component system. The effect of the reaction mixture composition (C_3H_8, NH_3 and O_2) on selectivity towards different products was studied at propane conversion above 80%. The favorable effect of bismuth promoter on the selectivity towards acrylonitrile was explained by suppression of acrylonitrile transformation connected with decreasing acidity of the catalyst.

Keywords: MoVTeNb oxide catalyst; Bi-doped, ammoxidation; propane; acrylonitrile.

1. Introduction

Direct oxidation of propane to acrylic acid or propane ammoxidation to acrylonitrile (ACN) is a promising alternative to their production from propylene. MoVTeNbO mixed oxide catalysts developed in the 90-s by Mitsubishi Chemical Corp. are efficient in the conversion of propane to acrylic acid and ACN [1-3]. The studies have been focused mainly on the chemical and phase composition of the catalysts, the structure of M1 and M2 phases, and the preparation methods [4-17]. Recent publications provide data on the nature of the active sites, the reaction mechanism and kinetics [4, 18-30].

The pathways of ACN formation via propylene have been established for catalysts of various phases and stoichiometric compositions [21-25]. More detailed kinetic studies of the ammoxidation of propane on MoVTeNb were described elsewhere [30-32]. According to Asakura et al. [30], ACN is formed directly from propane rather than through intermediate propylene. The rate of propane ammoxidation to ACN is described by an empiric power equation; the reaction rate increases at raising the concentrations of oxygen and propane while ammonia influences negatively. The effect of the reaction mixture composition on the rate of reaction on $Mo_1V_{0.4}Nb_{0.1}Te_{0.2}O_x$ catalysts was studied earlier [31]. The acrylonitrile yield of 53% was achieved at 703 K using a feed containing propane, ammonia and air at 1/1.2/15 ratio. The parallel and consecutive pathways of the reaction products formation on the $MoV_{0.3}Nb_{0.12}Te_{0.17}O_x$ catalyst according to previous studies [32] are shown on Scheme 1. The first order rate constants were calculated in accordance with the proposed mechanism. The slow step in the ACN formation is the propane activation ($k_1 = 0.81$). There are two routes of ACN formation; ACN is formed directly from propane and via propylene.

The rate of propylene conversion to ACN is more than an order of magnitude higher than that of propylene formation; the reaction rate constant ratio is $k_2/k_1 = 13$. The comparison of the rate constants of CO_x formation from ACN, propylene and propane ($k_3 = 0.46$, $k_4 = 4.20$, $k_5 = 0.02$) shows that the complete propylene oxidation is the fastest of the three. Comparison of the rate constants of parallel propylene conversion to CO_x and ACN, $k_4/k_2 = 0.4$, suggests that substantial share of ACN selectivity is lost due to the deep propylene oxidation.

For the majority of MoVTeNb catalyst systems, initial selectivity towards propylene can achieve 80% or greater value. The ACN selectivity in the middle conversion range up to 80% is usually 65-70%. If the selectivity does not decrease at higher conversions, the ACN yield would be close to its selectivity. Apparently, the oxidation of ACN plays a significant role in the yield decrease. In the work cited above [32] the experiments were performed at conversions lower than 70%; at these conversions the ACN oxidation is not prominent. The propane ammoxidation should be reliably studied at considerably higher propane conversions to elucidate the reaction route of ACN

transformation. Increased ACN yield can be achieved preserving high selectivity by suppression of these routes.

According to the literature [33-35] and our opinion [36], the direction of hydrocarbons transformation to the selective oxidation or to the deep oxidation depends on the bond strength of the surface compounds of reactants and products. Weak products binding provides a high rate of the desorption preventing the deep oxidation or degradation. The bond strength of surface complexes depends on the acid-base properties of the reactant and the catalyst. The conception of the acid-base interactions between gaseous reactants and surface sites of the solid catalysts was developed by Stair [37]. Doping is an effective way to change the acid-base properties of the catalyst. Introduction of electronegative elements onto the surface should produce an inductive effect making the nearby metal cations less basic or more acidic. Introduction of electropositive species such as alkali elements should produce a more basic or less acidic sites [37]. Grasselli hypothesized that acidic elements (e.g. P, B, W) should enhance the acidic properties of $Mo_1V_{0.31}Nb_{0.12}Te_{0.2}$ catalysts whereas basic elements (e.g. Cs) should enhance basic properties. The elevation of acidity in the first case should enhance the selectivity towards acrylic acid. Contrariwise, the enhancement of basic properties in the second case should decrease the selectivity towards acrylic acid. Indeed, the addition of P results in the increase the selectivity towards acrylic acid, whereas the addition of Cs depresses significantly the formation of acrylic acid. [38]. The incorporation of potassium in Mo–V–Sb–O catalysts result in a significant decrease in the number of acid sites on the catalyst surface favoring the formation of acrylic acid on the redox sites and decreasing the formation of acetic acid on the oxyhydrative scission acid sites in the oxidation of propane [39-41]. Baca et al. [42] found a correlation between acidity of the M1 phase promoted with Nb in MoVTe(Sb)O catalysts and selectivity in the oxidation of propane. Surface acidity strongly affects the binding and reactivity of propene molecules which have a basic character. Lowering the amount of strong Lewis acid sites (LAS) or Brønsted acid sites (BAS) increases the selectivity towards acrylic acid due to a reduction in the deep oxidation of propylene to CO_x on LAS or due to a decline in the acetic acid and acetone formation on BAS. Lopez-Medina et al. [22] demonstrated that Te^{4+} in nanostructured $MoVNbTe/Al_2O_3$ catalyst decreases the amount of strongly acidic sites. It results in increasing the selectivity towards acrylic acid due to reducing the number of strongly bound carboxylate complexes. The latter are intermediates of deep oxidation products. The higher selectivity towards acrylic acid over Ga-containing MoVTeO catalysts has been related to modifying acid properties of the catalysts surface. The presence of Ga^{3+} cations on the catalysts surface decreases the number and the strength of acid sites favoring the selective oxidation of propane to acrylic acid [43]. The acidity of the active sites has a strong influence on selectivity of the MoVTeNbO catalysts in both the oxidation and the ammoxidation of propane. Centers with moderate acidity favor to the partial oxidation where as

strong acid sites advantage the deep oxidation. Steam or ammonia during the oxidation or ammoxidation reactions, respectively, block the strong LAS and promote selective course of the reactions [17].

In general, we can conclude that the strong acidity of active centers leads to the formation of side products. Deep oxidation products are formed on LAS, whereas oxyhydrative scission products are generated on BAS.

Cited above works associate acidity and selectivity towards acrylic acid through the influence on the transformation of the intermediate propylene. The effect of the acidity on the transformation of final products is equally important. But such data both on acrylic acid in the oxidation of propane and on acrylonitrile in the ammoxidation of propane are absent.

ACN is organic base due to the presence of unshared electron pair on the nitrogen atom. It interacts with acid sites by donation of the electron density from the nitrogen atom [37]. The MoVTeNb oxide catalyst contains highly electronegative elements in the highest oxidation state ensuring the catalyst acidity. Reducing the acidity of active centers by introduction electropositive supplements should lead to a decrease in the bond strength of the adsorbed acrylonitrile preventing the oxidation and the oxidative scission of surface species.

As a promoter, we have chosen Bi, firstly as a more electropositive element in comparison with the basic composition of MoVTeNb catalyst and secondly as an indispensable component of industrial catalysts for the ammoxidation of propylene and the oxidation of propylene to acrolein in a two-stage production of acrylic acid.

In this study, we attempted to promote the MoVTeNb oxide catalyst with Bi in an effort to control of acrylonitrile conservation. The object of our study was the reaction pathways of propane ammoxidation on the $Mo_{1.2}V_{0.3}Te_{0.23}Nb_{0.12}O_x$ and Bi-modified catalysts, and the effect of the reaction mixture composition at propane conversion above 80%.

2. Experimental

2.1. *Catalyst preparation*

The $Mo_{1.2}V_{0.3}Te_{0.23}Nb_{0.12}O_x$ catalyst was prepared using ammonium heptamolybdate $(NH_4)_6Mo_7O_{24}\times 4H_2O$, ammonium metavanadate NH_4VO_3 (chemicals from commercial suppliers in Russia) and telluric acid H_6TeO_6 (Aldrich); the purity of each reagent was 99% or higher. Niobium oxalate was prepared by hydrolysis of niobium pentachloride ($NbCl_5$, Acros Organics, 99.8%) in water and neutralization with ammonium hydroxide (NH_4OH). White precipitate was filtered, washed with water and dissolved in a solution of oxalic acid ($C_2O_4^{2-}$/Nb = 3.0).

The catalysts were synthesized from slurry according to the patented procedure [1]. First, the aqueous solution of molybdenum, vanadium and tellurium compounds was prepared. Then, niobium oxalate

was added to the ternary solution. After addition of niobium oxalate solution pH of the catalyst slurry was 2.9. Solid precursor powder was prepared by spray-drying of the slurry in a laboratory spray-dryer (Buchi-290), the inlet temperature was 220 °C and the outlet temperature was 110 °C. The resulting powder was calcined for a short period in air at 300 °C and in a He flow at 600 °C for 2 h.

The $Mo_1V_{0.3}Te_{0.23}Nb_{0.12}Bi_nO_x$ (n = 0.01 - 0.05) catalyst was prepared by mixing powders of $Mo_1V_{0.3}Te_{0.23}Nb_{0.12}O_x$ and Bi_2O_3. The product was calcined at 550 °C in He flow for 2 h. The calcined powders were pressed into tablets, crushed and then sieved. The 0.25-0.50 mm fraction was used in the experiments.

2.2. *Catalyst characterization*

The specific surface areas of the catalysts were determined by low temperature nitrogen adsorption at 77 K using an automatic ASAP-2400 apparatus.

The phase composition of the catalysts was studied using a Siemens D500 diffractometer. Scanning was performed in the 2θ range from 5° to 70° with a step of 0.028° using Cu *Kα* radiation (λ = 1.5418 Å).

The chemical composition of the catalysts was determined by X-ray photoelectron spectroscopy (XPS) using a SPECS's Surface Nano Analysis GmbH spectrometer equipped with a PHOIBOS-150 hemispherical electron energy analyzer, a FOCUS-500X-ray monochromator and an XR-50M X-ray source with a double Al/Ag anode. The core-level spectra were obtained using the monochromatic Al *Kα* radiation under ultrahigh vacuum conditions. Binding energies of the photoemission peaks were corrected to the C1s peak (284.8 eV) from the adventitious contaminated layer. Relative element concentrations were determined from the integral intensities of XPS peaks using the cross-sections according to Scofield.

The thermal programmed desorption (TPD) of ammonia in combination with IR spectroscopy was applied to characterize the acidity of the samples. FTIR spectra were obtained with a BOMEM MB-102 spectrometer. The spectrometer was operated in the transmission mode using a specially designed quartz cell-reactor with BaF_2 windows. The catalysts were pressed into a thin self-supporting pellet (15 mg/cm^2) and placed into the cell-reactor. The FTIR experiments were performed at atmospheric pressure using a feed of 5 vol% NH_3 in a He flow. The spectra were measured at 25–300 °C in a range of 2000–1000 cm^{-1} at a resolution of 4 cm^{-1}. The samples were preliminarily activated in a flow of air for 60 min at 300 °C. Subsequently, the cell-reactor and the catalyst sample were cooled to 25 °C, and the air flow was replaced by the ammonia containing mixture flow. The IR spectra were measured during the adsorption. After constant surface covering was achieved, the ammonia containing mixture flow was replaced by a He flow. Then the

temperature was increased at a rate of 1 °C/min. The IR spectra were collected at selected temperatures during the TPD experiments.

2.3. *Catalytic tests*

The catalytic tests were carried out at atmospheric pressure in a tubular flow fixed bed reactor (i.d. 12 mm; length 50 mm) with a coaxial thermocouple pocket (i.d. 4 mm). Samples (0.25–0.50 mm particle size) were diluted with an inert material and charged into the reactor. The reactor was kept in an air heated furnace. The temperature change along the furnace height was ±2 °C. The reaction temperature was measured using a thermocouple placed in the thermocouple pocket directly in the catalyst bed. Before operation, the catalyst was heated in a helium flow to the required temperature.

The catalysts were compared at a constant composition of the reaction mixture with a molar ratio $C_3H_8/NH_3/air$ = 1/1.2/15 at 420 °C. Kinetic studies were performed at different reaction mixture compositions and contact times. The later was changed by variation of the catalyst weight or the flow rate.

3. **Results and discussion**

3.1. *The composition and structure of the catalysts*

Table 1 summarizes the chemical composition of the samples under study before and after calcination as well as their specific surface area. Tellurium loss due to sublimation is the main reason for the difference in composition of calcined and uncalcined samples. According to the XRD analysis all samples consist of the orthorhombic phase M1, the hexagonal phase M2, $TeMo_5O_{16}$ and $(V_{0.07}Mo_{0.93})_5O_{14}$.

The complexity of the chemical composition and small amounts of additives hinder the identification of structural differences of promoted and unpromoted catalysts. To study the phase composition, we used XRD and IR spectroscopy. XRD patterns are typical for M1 and M2 phases (Fig. 1). IR spectra obtained (not shown) are also not original [44] and entirely confirm the XRD data.

Fig. 1 shows the XRD patterns of the calcined catalysts. The 2θ peaks at 6.6, 7.9, 9.0, 22.1 and 27.2º are assigned to the orthorhombic phase M1 and the 2θ peaks at 22.1, 28.2, 36.2 and 45.15º are assigned to the M2 phase. In addition, the weak reflections of $TeMo_5O_{16}$ (peaks at 21.7, 24.6, 26.2, 26.7, 30.5 and 34.9º) [JCPDS, 31-874] and $(V_{0.07}Mo_{0.93})_5O_{14}$ (peaks at 22.2, 23.4, 25.0 and 31.5º) [JCPDS, 31-1437] are also observed. Introduction of bismuth in the Bi/Mo ratio of 0.01–0.02 results in a minor increase in the amount of the M2 phase. The sample with the atomic ratio Bi/Mo of 0.05 comprises a lot of the hexagonal phase M2.

According to the XPS analysis, the samples contain Mo, V, Nb, Te, Bi, and O. Corresponded core-level spectra of the $Mo_1V_{0.28}Te_{0.14}Nb_{0.13}$ and $Mo_1V_{0.28}Te_{0.18}Nb_{0.11}Bi_{0.01}$ catalysts are presented in Fig. S1 of supporting material. The $Mo3d_{5/2}$, $Te3d_{5/2}$, $Nb3d_{5/2}$, $V2p_{3/2}$, $Bi4f_{7/2}$ and O1s binding energies are summarized in Table 2. In both the cases the Mo3d spectra consist of two symmetric peaks corresponded to the $Mo3d_{5/2}$ – $Mo3d_{3/2}$ spin-orbit doublet. The $Mo3d_{5/2}$ binding energy is in the range 233.1-233.2 eV that is typical of molybdenum in the Mo^{6+} state [45]. The $Te3d_{5/2}$ spectra consist of a sharp peak at 576.8-577.0 eV that is also typical of Te in the highest oxidation state Te^{6+} [46]. The Nb3d core-level spectra contain well-defined $Nb3d_{5/2}$ – $Nb3d_{3/2}$ spin-orbit doublet. The $Nb3d_{5/2}$ binding energy is in the range 207.3-207.4 eV that can be attributed to the Nb^{5+} state. Bulk Nb_2O_5 is characterized by the $Nb3d_{5/2}$ binding energy equal to 207.8 eV [47]. In the $V2p_{3/2}$ spectrum of $Mo_1V_{0.28}Te_{0.14}Nb_{0.13}$ the wide peak at 517.0 eV is observed. The doping by Bi leads to a shift the peak to 517.2 eV. Both these values correspond to the V^{5+} state [48]. The Bi4f spectrum consist of two sharp peaks at 159.9 and 165.2 eV which correspond to the $Bi4f_{7/2}$ – $Bi4f_{5/2}$ spin-orbit doublet (not shown). According to the literature [49], Bi^{3+} is characterized with the similar values of the $Bi4f_{7/2}$ binding energy in the range of 159.3-159.9 eV. The atomic ratio [Bi]/[Mo] is equal to 0.011 that is in good agreement with the results of chemical analysis (Table 1).

Table 3 demonstrates the surface content of the elements with respect to the surface content of Mo.

One can see that on the surface of the promoted sample, the V content is significantly higher, the Te content is considerably reduced, whereas the Nb content is virtually unchanged. XPS results show also the correspondence between surface and bulk Bi content of promoted sample. It confirms clearly the introduction of Bi in M1 phase structure.

Our high-resolution transmission electron microscopy studies [50] identified no new phases induced by the bismuth addition. Bismuth addition also does not change the structure and morphology of the M1 phase.

Previously, Grasselli et al. [38] studied the promotion of MoVNbTe catalyst by small additives of phosphorus (P/Mo = 0.01, 0.001). They emphasized that the dopants concentration must be kept critically low for the success of the catalysis. The authors also found no change in the structure of the phases and suggested that phosphorus is located in the heptagonal or hexagonal channels of the M1 and M2 phases. Taking into account our XPS data, we [50] also assume that Bi is localized in the six- and seven-membered channels of the M1 structure similar to its chemical analog Sb [12] or P [38].

3.2. Catalytic performance

Catalytic characteristics of the samples containing different amounts of bismuth are shown in Table 4. Samples with atomic ratio Bi/Mo = 0.01–0.02 are more active than the standard sample. We

associate the decrease in the overall catalysts activity after introduction of a larger amount of bismuth (Bi/Mo = 0.05) with the formation of M2 phase, which is more than an order of magnitude less active than the M1 phase both in the propane and in the propylene oxidation [51]. In the region of propane conversions above 90%, the selectivity towards acrylonitrile obtained on the Bi-modified catalysts is much higher than that obtained on the non-modified samples. The modified samples also show a lower activity in the oxidation of ammonia and in the oxidation of propane into carbon oxides. As mentioned above, the introduction of a larger amount of bismuth (Bi/Mo = 0.05) decreases the overall catalysts activity as well as the selectivity towards ACN. Let us note that the M2 phase contains more reactive weakly bound oxygen than the M1 phase [52], and this contributes to the reduction of a selectivity toward ACN in the case of the sample with Bi/Mo = 0.05.

The selectivities towards C_3H_3N, C_3H_6, CO_x, C_2H_3N+HCN, and $C_3H_4O_2$ as a function of the propane conversion on the $Mo_1V_{0.28}Te_{0.14}Nb_{0.13}O_x$ and $Mo_1V_{0.28}Te_{0.18}Nb_{0.11}Bi_{0.01}O_x$ catalysts are shown in Fig. 2. The major products of the selective conversion of propane on both catalysts are acrylonitrile and propylene. By-products include acetonitrile, HCN, acrylic acid, and CO_x. The dependence of selectivity on conversion is the same for both catalysts when conversion is in the range of 20-80%. As the propane conversion increases from 20 to 40%, selectivity towards C_3H_6 decreases from about 22% to 10%, and the selectivity towards acrylonitrile increases from 53% to 67%.

Selectivity towards CO_x continuously increases with the increase of the conversion of propane. Selectivity towards acetonitrile and HCN are fairly constant at 20-80% propane conversion. At the conversion of propane higher than 80%, a notable difference between the unmodified and modified catalysts is observed. In the case of the $M_{0.1}V_{0.3}Te_{0.14}Nb_{0.13}O_x$ catalyst, an increase in the propane conversion to 93% leads to a dramatic decline in the selectivity towards acrylonitrile from 67% to 40%. On the modified catalyst, the selectivity towards acrylonitrile decreases only to 56%. The decline in selectivity towards acrylonitrile is accompanied by the increase in selectivities towards CO_x, acrylic acid and acetonitrile.

Therefore, the selectivity towards acrylonitrile on the modified catalyst is comparable to that on the non-modified sample at the propane conversion up to 80% and is much higher in the region of the propane conversions above 80%.

3.3. Effect of the reaction mixture composition

Reaction products in the ammoxidation of propane are acrylonitrile, oxidation products (acrylic acid and COx) and oxidative scission products (HCN and C_2H_3N). With increasing the propane conversion, an intensive conversion of ammonia takes place simultaneously, and the direction of the reaction is shifted towards the oxidation and the oxidative scission. In Oliver et al. opinion [17], in the propane ammoxidation, the optimal amount of ammonia should depend on conversion level.

Thereby, the maintenance of the optimal composition of the reactant mixture is particularly important at the high propane conversion.

The effect of the reactant mixture composition on the catalytic performance was studied over the $Mo_1V_{0.28}Te_{0.18}Nb_{0.11}Bi_{0.01}O_x$ catalyst at the high propane conversion level (higher than 90%). Monoparametric experiments were performed by changing the content of a certain component in the reactant mixture while the concentrations of the other components were held constant. Figures 3a, b, and c show the results of the experiments.

3.3.1. Effect of propane concentration

The concentration of propane in the reactant mixture was varied from 4 to 7% at the constant concentrations of oxygen and ammonia (18.5% and 7%, respectively) and the contact time equal to 3.0 s. The experimental results are shown in Fig. 3a.

As the concentration of propane increases from 3.5 to 7% the propane conversion decreases from 93.8 to 89.2%. The selectivity towards ACN passes through a small maximum (58.6–58.1%) at the propane concentration 5–5.3%. At the propane concentration below 5%, the selectivity towards ACN decreases due to increased formation of deep oxidation products, while at the propane concentration above 5.3%, this is occurred due to elevated formation of acetonitrile. An increase in the selectivity towards propylene from 0.1 to 0.7% in the region of high propane concentrations is due to lower conversion of propane. As the propane concentration increases, the selectivity towards hydrocyanic acid decreases steadily from 1.7 to 0.9%. The selectivity towards acrylic acid varies only slightly in the range of propane concentrations under consideration.

3.3.2. Effect of ammonia concentration

The concentration of ammonia in the reactant mixture was varied from 4.5 to 10.2% at the constant concentrations of propane and oxygen (5.0% and 19%, respectively) and the constant contact time of 3.4 s. The experimental results are shown in Fig. 3b.

As the ammonia concentration increases from 4.5 to 10%, the propane conversion decreases from 96 to 90%. The selectivity towards ACN at the propane conversion 95–96% changes from 46.1 to 56% as the ammonia concentration increases from 4.5 to 6%, and then declines to 54.8% as the ammonia concentration further increases to 10.2%. A decrease in the selectivity towards ACN in the region of high ammonia concentrations is accompanied by an increase in the acetonitrile concentration.

At high concentration of ammonia, there is a considerable (approximately 4-fold) decrease in the selectivity towards acrylic acid and carbon oxides. The selectivity towards HCN remains virtually constant (1.5%) in a range of the ammonia concentrations 4.5–6.8% and decreases to 0.3% at further

increase in the ammonia concentration. In the region of high ammonia concentrations, the propane conversion declines, and the selectivity towards propylene increases from 0.3 to 0.8 %.

3.3.3. Effect of oxygen concentration

The concentration of oxygen in the feed mixture was varied from 14.3 to 23.6% at the constant concentrations of propane and ammonia (5.0% and 6.0%, respectively) and the contact time 3.2 s). The experimental results are presented on Fig. 3c.

The elevation of the oxygen concentration from 14.3 to 23.6% leads to an increase in the propane conversion from 85.9 to 94%. The selectivity towards acrylonitrile passes through a maximum (about 56%) in a range of the oxygen concentrations 17–19%.

As the oxygen concentration decreases from 17 to 14.3%, the selectivity towards ACN also decreases and the selectivity towards acetonitrile increases. When the oxygen concentration exceeds 18.7%, the selectivity towards carbon oxides and acrylic acid starts to increase. The selectivity towards hydrogen cyanide changes slightly in a range of the oxygen concentrations 16–23.6%. The selectivity towards propylene decreases as the oxygen concentration changes from 14.3 to 16% and remains constant at higher oxygen concentration.

Processing of all series of monoparametric experiments in “acrylonitrile yield versus the ratio of component concentrations” coordinates allows determining the condition that provides the maximum yield of the target product (fig. 4).

The yield of acrylonitrile passes through a maximum in a range of the O_2/C_3H_8 ratio 3.4–3.6. At lower values of the O_2/C_3H_8 ratio, the yield of acrylonitrile decreases due to increased formation of acetonitrile, while at higher values this is due to increased formation of acrylic acid and carbon oxides.

The maximum yield of acrylonitrile is observed in a range of the O_2/NH_3 ratio between 2.7 and 3.1 and decreases at higher values of the O_2/NH_3 ratio due to increased formation of propane oxidation products, acrylic acid and carbon oxides.

The yield of acrylonitrile passes through a maximum in a range of NH_3/C_3H_8 ratio between 1.2 and 1.4. At the NH_3/C_3H_8 ratio below 1.2, the yield of acrylonitrile decreases due to increased formation of acrylic acid and CO_x. At the NH_3/C_3H_8 ratio above 1.4, the yield of acrylonitrile declines due to increased formation of acetonitrile and carbon oxides.

Therefore, the kinetic experiments determined quite narrow intervals for optimal ratios of the feed mixture components at high conversion level.

Typically, in the academic literature, air is used as an oxidizer; the rest is in accordance with the objectives of the study. To compare the samples, we traditionally used in our work the mixture with ratio of $C_3H_8/NH_3/air$ = 1/1.2/15. This composition is the most common in the literature also. The ratio corresponds to $C_3H_8/NH_3/O_2$ ratio = 1/1.2/3, which is within the range of optimal C_3H_8/NH_3 and NH_3/O_2 ratios. The C_3H_8/O_2 ratio appears significantly below the optimum (3 vs 3.5). Therefore, at high propane conversion, it is necessary to dose oxygen apparently due to the high degree of the catalyst reduction under reaction conditions. The optimal components ratios are the concentration ranges. This gives a certain freedom in the independent variation of reactant mixture components. Concerning the industrial process [53], the composition of the reaction mixture is not reported, but our recommendations are the same. We believe that these recommendations are useful also for process with recycle [54].

4. Discussion

Dependence of selectivities towards different products in the propane conversion (Fig. 2) can be described by the parallel-consequential network of the ammoxidation reaction mechanism. The fact that the selectivity towards acrylonitrile increases as the selectivity towards propylene decreases, suggests a consecutive (via propylene) mechanism of acrylonitrile formation. Products of total oxidation (CO_x) form directly from propane (selectivity ca.15% at $X \rightarrow 0\%$) and also from propylene and acrylonitrile. A drastic decrease in the selectivity towards acrylonitrile and increase in the selectivity to CO_x and acetonitrile at the propane conversions greater than 80% indicates the predominant reaction pathway of these products formation is acrylonitrile transformation. The formation of CO_x from propylene is less significant, which is evidenced by only a small change in the selectivity towards CO_x at intermediate propane conversions.

The promotion of the MoVTeNbO catalysts with Bi does not affect the proportion of formation of products from the parallel route from propane and propylene, however decreases acrylonitrile transformation.

Fig. 5 illustrates a positive effect of bismuth addition on the acrylonitrile yield. The modification of the catalyst with Bi results in increasing the yield of acrylonitrile as compared to the four-component catalyst at high conversions. Therefore, the incorporation of bismuth leads to an increase of the acrylonitrile yield due to decline in the ACN transformation.

It is impossible to explain the improvement in the catalytic performance by structural features of the promoted catalyst. Reduced transformation of ACN on the MoVTeNbBi catalyst could be caused by the modification of the surface acid properties. The thermal programmed desorption (TPD) of ammonia in combination with IR spectroscopy was applied to characterize the acidity of the samples.

The adsorption of ammonia at room temperature on the samples both with and without bismuth results in the appearance of the single band at about 1410 cm^{-1} in the 2000-1000 cm^{-1} region of infrared spectra. The band could be assigned to the $\delta_{as}(NH_4^+)$ mode of adsorbed ammonium ions formed by the interaction of ammonia molecules with Brønsted acid sites. The intensity, position of maximum and width of the band under steady state are only slightly dependent on the presence of bismuth in the samples. Fig. 6 demonstrates the dependence of the relative coverage of the surface with ammonium ions on the temperature during the TPD experiments. The surface covering measured at room temperature is adopted as 1. Decreasing the intensity of the $\delta_{as}(NH_4^+)$ band is observed with increasing temperature. The bismuth incorporation reduces the temperature of desorption start at approximately 50 °C and increases the desorption rate, particularly at 120-180 °C. In the case of Bi containing sample, complete desorption of ammonium proceeds also at a lower temperature. Temperature shift of the desorption is a measure of the strength of the acid sites [55]. In the presence of Bi, approximately a 10 cm^{-1} low-frequency shift of the band is also observed during temperature increase. Thus, in this case the band position depends on the surface covering. In the absence of Bi**,** the maximum of the band does not depend on the surface coating. Thus, the presence of bismuth in the catalyst lowers the strength of the Brønsted acid sites.

It is important to note that despite the high electronegativity of elements constituting the catalyst, the strength of Lewis acid sites is small, since we have failed to detect any bands characterizing surface species of pyridine and ammonia with Lewis acid sites in IR spectra of both quaternary catalyst and that of the catalyst promoted with bismuth. We have failed to measure the spectrum of adsorbed pyridine (relatively weak base). This is in agreement with the work [41]. Thus, the surface of the catalysts is insufficient acidic to adsorb a weak base. However, ACN has a basic nature due to the unshared electron pair of nitrogen [37]; and an interaction of ACN and a catalyst is an indicator of active center acidity. In accordance with [17, 22], highly acidic LAS are sites of adsorption of strongly bound surface species which are intermediates of the deep oxidation products. The decrease in the selectivity towards products of the deep oxidation of acrylonitrile is an evidence of itself of decline LAS acidity.

The promotion of MoVTeNb oxide catalyst composed of highly electronegative elements by less electronegative bismuth decreases the acidity of active sites and even more weakens the binding of acrylonitrile with active centers reducing its degradation and oxidation. At the same time, the reduced selectivity toward acetonitrile and HCN is a result of the decrease of the strength of Brønsted acid sites responsible for oxyhydrative scission [17, 22, 55].

It should be noted that the promotion of the catalyst with bismuth does not affect the transformation of propylene. We attribute this fact to relatively low basicity of the Bi, which is insufficient to adequately reduce the acidity of the active sites binding propylene strongly. Analyzing the value of

the ratio of the rate constants of parallel propylene conversion routs to CO_x and ACN ($k_4/k_2 = 0.4$) [32], we can conclude that substantial share of propylene is strongly bound. To sufficiently reduce the acidity of these centers, the catalyst must be doped with the element, which is more basic than the Bi. The Ga^{+3} can be an example of such a promoter. On the samples doped with Ga, a sharp increase in selectivity toward acrylic acid is occurred at low propane conversions (X < 10%) [43]. This region is characterized by the conversion of propylene into acrylic acid and COx [32]. The increase in selectivity toward acrylic acid can be attributed to inhibition of propylene parallel conversion into COx caused by a decrease in strength of propylene binding by less acidic active centers. Unfortunately, the introduction of Ga results in an increase in the acrylic acid conversion into the by-products. The maximum of selectivity toward acrylic acid is observed at 20-40% propane conversion for different samples. Increased conversion is accompanied by COx and acetic acid formation. Apparently, Ga reduces the acidity (increase the basicity [37]) too strongly. It leads to stronger acrylic acid binding and as result to degradation of the surface intermediates. In summary, "the nature and strength of acid sites should be tailored in order to optimize allylic oxidation and to avoid oxidative breaking of CC bonds" [29]. The promotion of well-known multicomponent MoBiCoFeNi PKO catalyst of propylene oxidation into acrolein and propylene ammoxidation into ACN with both acidic and basic additives is a good illustration.

The second effect of bismuth addition consists in a lowered activation of ammonia. Direct experiments have demonstrated a higher activity of the MoVTeNb oxide catalyst in the ammonia oxidation as compared to the bismuth modified catalyst (Table 4). This corresponds to reduced activity of the BiMo catalyst as compared to the activity of the MoVTeNb oxide catalysts in the direct oxidation of ammonia [31]. Along with the data of TPD of ammonia, this also supports the idea that the bismuth incorporation decreases the acidity of active sites.

Introduction of small amounts of Bi increases an activity in the propane ammoxidation (Table 4). We attribute this fact to a change in the surface composition of the catalyst. By XPS, we have established the correspondence between the bulk and surface bismuth content in promoted sample. We also found an increase in vanadium, a decrease in tellurium, and constancy of niobium content on the surface of promoted sample as compared to unpromoted one (Table 3).

A comparison of the catalytic properties and XPS data shows the general trend in the change of vanadium surface content and an activity of the catalysts in the conversion of propane. The ratio of surface concentration $V^{5+}{}_{Bi}/V^{5+}$ (1.27) is very close to the ratio of rate constants k_{Bi}/k (1.33).

The formation of ACN on MoVTeNbO M1 phase proceeds through intermediate oxidative dehydrogenation of propane. In this reaction, the limiting rate-determining step is the H abstraction.

The V^{5+}=O acid-base pair participates in the activation of propane by V^{5+} centers and in the H abstraction by lattice oxygen according to a Mars-van Krevelen redox mechanism [56].

Our correlation between V^{5+} surface content and activity confirms that H abstraction from propane is the rate-limiting step and that V^{5+} on the surface of MoVTeNbO catalysts is the active site in propane activation.

The Mo-O-Te moieties are the centers of the allyl oxidation of propylene [51]. Since MoTe oxide system is active in the oxidation of propylene at a ratio of Te/Mo≤0.1 [57], the decrease of tellurium content (Table 3) is not critical.

Molybdenum is the main component in the M1 phase. In the Grasselli mechanism [12], Mo is the center where the interaction of C3 fragments and ammonia is occurred resulting in ACN formation. In accordance with the principles of acid-base interaction of the reactants and catalyst cations [37], Mo^{6+} must be a center of the strong binding of ACN; the reduction in the Mo oxidation state (acidity) weakens the binding. Indeed, in the Grasselli mechanism, ACN is desorbed unchanged from Mo in the reduced state [12]. Thus, the weak binding of the surface acrylonitrile intermediate provides a high selectivity of MoVTeNb catalyst in the reaction under consideration.

The target product preservation is a common problem of selective oxidation. A strong re-absorption of a target product under a reaction conditions leads to its transformation. A modification of catalysts should be directed to the active site of a possible re-adsorption of the product in order to weaken its bond strength. In case of the formation of acidic product, promoter should increase the acidity of the active center (see, e.g. [58]). Contrariwise, in the case of a basic product, promoter should reduce the acidity (increase the basicity) of the active center. The main effect of bismuth is to decrease the acidity of the active sites. This prevents strong binding of re-adsorbed acrylonitrile and subsequent degradation of the carbon skeleton. The latter results in COx, HCN, and acetonitrile formation.

Let us note that it is reasonable to use the target product transformations reactions as test ones when selecting promoter.

5. Conclusion

The ammoxidation of propane on the MoVTeNb catalyst proceeds with a high selectivity at conversions less than 80%. At higher conversions, the selectivity towards acrylonitrile decreases due to its further oxidation and oxyhydrative scission. Undesired reactions may be suppressed by the addition of elements with a basic character to the catalyst.

All the components of the MoVTeNb oxide catalyst are highly electronegative elements that determine acidic properties of the catalyst active sites. The promotion by bismuth decreased the

acidity of active sites of acrylonitrile activation and slows down its further transformation. The second key factor is a low catalyst activity in the oxidation of ammonia. The addition of bismuth decreases the activation and suppresses the oxidation of ammonia. As result, the NH_3/C_3H_8 ratio retains close to desired values over the entire range of the propane conversions. This favors the target product formation and a high selectivity at the propane conversion above 90%. The promotion by bismuth results in increasing the yield of acrylonitrile as compared to that of the four-component catalyst.

A high conversion of propane is a crucial parameter for industrial processes. The composition of reactant mixture at high conversions strongly effects on the yield of acrylonitrile. The influence of propane, ammonia, and oxygen on the activity and selectivity of the MoVTeNbBi oxide catalyst was studied. The ratios of components concentration are crucial for the ACN yield. The optimal ratios appear to be in narrow ranges: NH_3/C_3H_8 = 1.2–1.4, O_2/C_3H_8 = 3.4–3.6, O_2/NH_3 = 2.7–3.1. Maintenance of these ratios in the reactant mixture via feeding appropriate components in a industrial reactor [53] or into a gas recycle stream [54] maybe an effective technique for the enhancing productivity of the process.

Acknowledgment. This work was partially supported by the Ministry of Education and Science of the Russian Federation. The authors gratefully acknowledge the support by the Federal Special Program "Scientific and Educational Cadres of Innovative Russia" (2009-2013) and Russian Foundation for Basic Research (the research project No. 11-03-00584-a). We thank Dr. Aleshina for help in the preparation of catalysts and Prof. Plyasova for the XRD measurements.

References

1. M. Hatana, A. Kayou, US Patent 5,049,692 (1991); T. Ushikubo, K. Oshima, T. Ihara, H. Amatsu, US Patent 5,380,933 (1995), Assigned to Mitsubishi Chemical Co.
2. T. Ushikubo, K. Oshima, A. Kayou, M. Vaarkamp, M. Hatano, J. Catal. 169 (1997) 394-396
3. M. Lin, M. Linsen, US Patents 6,180,825 (2001); 6,514,901 (2003); 6,514,903 (2003) and Patent Application EP 962,253 (1999).
4. T. Ushikubo, K. Oshima, A. Kayo, M. Hatano, Stud. Surf. Sci. Catal. 112 (1997) 473- 480.
5. P. De Santo Jr., D.J. Buttrey, R.K. Grasselli, C.G. Lugmair, A.F. Volpe, B.N. Toby, T. Vogt, Z. Kristallogr. 219 (2004) 152-165.
6. J. Holmberg, R.K. Grasselli, A. Andersson, Top. Catal. 23 (2003) 55-63.
7. H. Tsuji, K. Oshima, Y. Koyasu, Chem. Mater. 15 (2003) 2112-2114.
8. P. Botella, E. García-González, A. Dejoz, J.M. López Nieto, M.I. Vazquez, J. M. González-Calbet, J. Catal. 225 (2004) 428-438.
9. H. Murayama, D. Vitry, W. Ueda, G. Fuchs, M. Anne, J.L. Dubois, Appl. Catal. A 318 (2007) 137-142.
10. P. Botella, E. García-González, J.M. López Nieto, J. M. González-Calbet, Solid State Sci. 7 (2005) 507-519.
11. D. Vitry, Y. Morikawa, J.L. Dubois, W. Ueda, Top. Catal. 23 (2003) 47-53.
12. R.K.Grasselly, J.D. Burrington, D.J. Buttrey, P. Desanto Jr., C.G. Lugmair, A.F. Volpe Jr., T. Weingand, Top. Catal. 23 (2003) 5-22.
13. M. Baca, M. Aouine, J.L. Dubois, J.M.M. Millet, J. Catal. 233 (2005) 234-241.
14. J. Holmberg, R.K. Grasselli, A. Andersson, Appl. Catal. A 270 (2004) 121-134.
15. P. Korovchenko, N.R. Shiju, A.K. Dossier, U.M. Gram, M.O. Guerrero-Pérez, V.V. Guliants, Top. Catal. 50 (2008) 43-51.
16. W. Ueda, D. Vitry, T. Katou, Catal. Today 96 (2004) 235-240.
17. J.M. Oliver, J.M. López Nieto, P. Botella, Catal. Today 96 (2004) 241-249.
18. .P. Concepción, P. Botella, J.M. López Nieto, Appl. Catal. A 278 (2004) 45-56.
19. M.M. Lin., T.B. Desai, F.W. Kaiser., P.D. Klugherz, Catal. Today 61 (2000) 223-229.
20. W. Ueda and K. Oshihara, App. Catal. A 200 (2000) 135-143.
21. W. Ueda, K. Oshihara, D. Vitry, T. Hisano, Y. Kayashima, Catal. Surv. Japan 6 (2002) 33-44.
22. R. Lopez-Medina, I. Sobczak, H. Golinska-Mazwa, M. Ziolek, M.A. Ba˜nares, M.O. Guerrero-Perezc, Catal. Today 187 (2012) 195– 200
23. P. Botella, J.M. López Nieto, B. Solsona, A. Mifsud, F. Marquez, J. Catal. 209 (2002) 445-455.
24. J.M. López Nieto, B. Solsona, P. Concepción, F. Ivars, A. Dejoz, M.I. Vázquez, Catal. Today 157 (2010) 291-296.

25. W.A. Goddard III, K. Chenoweth, S. Pudar, A.C.T. van Duin, M.-J. Cheng, Top. Catal. 50 (2008) 2-18.
26. E. Balcells, F. Borgmeier, I. Grißtede, H.-G. Lintz, Catal. Lett. 87 (2003) 195-199.
27. E. Balcells, F. Borgmeier, I. Grißtede, H. -G. Lintz, F. Rosowski, App. Catal. A 266 (2004) 211-221.
28. R. K. Widi, S. Bee Abd Hamid, R. Schlogl, React. Kinet. Catal. Lett. 98 (2009) 273-286.
29. P. Concepcion, S. Hernandez, J.M. Lopez Nieto, Appl. Catal. A 391 (2011) 92–101.
30. K. Asakura, K. Nakatani, T. Kubota, Y. Iwasava, J. Catal. 194 (2000) 309-317.
31. M. Vaarkamp, T. Ushikubo, Appl. Catal. A 174 (1998) 99-107.
32. N. Watanabe, W. Ueda, Ind. Eng. Chem. Res. 45 (2006) 607-614
33. V.D. Sokolovskii, Catal. Rev.-Sci. Eng. 32 (1990) 1-49.
34. B. Grzybowska-Swierkosz, Top. Catal. 11/12 (2000) 23-42.
35. J. Haber, Catal. Today 142 (2009) 100-113.
36. T.V. Andrushkevich, Catal. Rev.-Sci. Eng. 35 (1993) 213–259.
37. P.C. Stair, J. Am. Chem. Soc. 104 (1982) 4044-4052.
38. R.K. Grasselli, C.G. Lugmair, A.F. Volpe Jr., Top Catal. 50 (2008) 66–73.
39. B. Solsona, V.A. Zazhigalov, J.M. Lopez Nieto, I.V. Bacherikova, E.A. Diyuk, Appl. Catal. A 249 (2003) 81–92.
40. F. Ivars, B. Solsona, P. Botella, M.D. Soriano, J.M. Lopez Nieto, Catal. Today 141 (2009) 294–299.
41. P. Botella, P. Concepcion, J.M. Lopez Nieto, B. Solsona, Catal. Lett. 89 (2003) 249-253.
42. M. Baca, A. Pigamo, J.L. Dubois, J.M.M. Millet, Catal. Commun. 6 (2005) 215-220.
43. S. Hernández-Morejudo, A. Mass, E. García-González, P. Concepción, J.M. López Nieto, Appl. Catal. A (2015) In Press doi:10.1016/j.apcata.2014.12.039
44. G.Ya. Popova, T.V. Andrushkevich, L.S. Dovlitova, G.A. Aleshina, Yu.A. Chesalov, A.V. Ishenko, E.V. Ishenko, L.M. Plyasova, V.V. Malakhov, M.I. Khramov, Appl. Catal. A: Gen. 353 (2009) 249–257
45. R.G. Kukushkin, O.A. Bulavchenko, V.V. Kaichev, V.A. Yakovlev, Appl. Catal. B 163 (2015) 531-538.
46. H. Hayashi, N. Shigemoto, S. Sugiyama, N. Masaoka, K. Saitoh, Catal. Lett. 19 (1993) 273-277.
47. D. Morris, Y. Dou, J. Rebane, C.E.J. Mitchell, R.G. Egdell, D.S.L. Law, A. Vittadini, M. Casarin, Phys. Rev. B 61 (2000) 13445.

48. V.V. Kaichev, G.Ya. Popova, Yu.A. Chesalov, A.A. Saraev, D.Y. Zemlyanov, S.A. Beloshapkin, A. Knop-Gericke, R. Schlögl, T.V. Andrushkevich, V.I. Bukhtiyarov, J. Catal. 311 (2014) 59-70.
49. C. Wang, C. Shao, L. Wang, L. Zhang, X. Li, Y. Liu, J. Colloid Interface Sci. 333 (2009) 242-248.
50. E.V. Ishchenko, A.V. Ishchenko, V.M. Bondareva, T.Yu. Kardash, V.I. Sobolev, T.V. Andrushkevich, Kinet. Catal. (2015) In Press
51. E.V. Ishchenko, G.Ya. Popova, T.Yu. Kardash, A.V. Ishchenko, L.M. Plyasova, T.V. Andrushkevich, Catal. Sust. Energ. 1 (2013) 75–81.
52. E. Sadovskaya, V. Goncharov, G. Popova, E. Ishchenko, D. Frolov, A. Fedorova, T. Andrushkevich, J. Molec. Catal. A: Chem. 392 (2014) 61–66
53. http://www.chemicals-technology.com/projects/-ptt-asahi-chemical-acrylonitrile-methyl-methacrylate/
54. J.F. Brazdil, Top. Catal. 38 (2006) 290-294.
55. M. Hävecker, S. Wrabetz, J. Kröhnert, L.-I. Csepei, R. Naumann d'Alnoncourt, Yu.V. Kolen'ko, F. Girgsdies, R. Schlögl, A. Trunschke, J. Catal. 285 (2012) 48–60.
56. V.V. Guliants, Catalysis 27 (2015) 33–61
57. T.V. Andrushkevich, G.K. Boreskov, L.L. Kuznetsova, L.M. Plyasova, Yu.N. Tyurin, Yu.M. Schekochihin, Kinet. Catal. 15 (1974) 424-429.
58. Z. Song, T. Matsushita, T. Shishido, K. Takehira, J. Catal. 218 (2003) 32–41.

Figure Captions

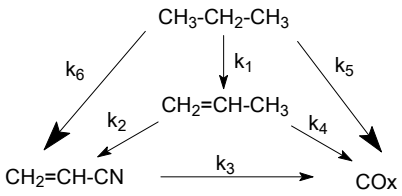

Scheme 1. Mechanism of propane ammoxidation [32].

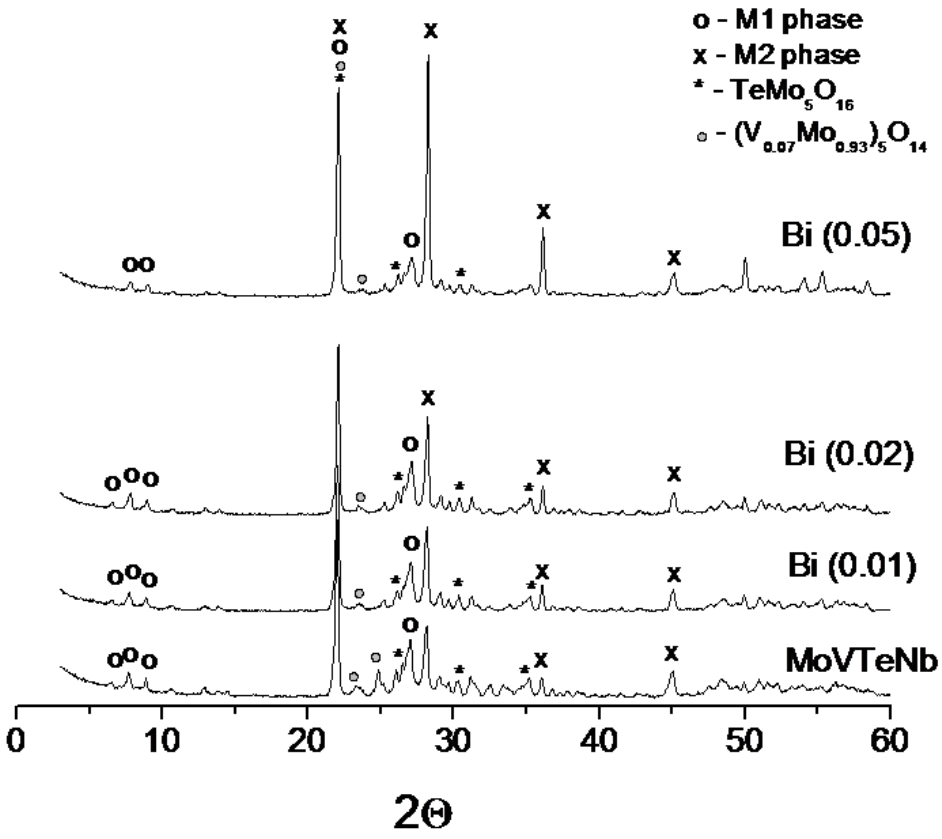

Fig. 1. XRD patterns of $Mo_1V_{0.28}Te_{0.14}Nb_{0.13}O_x$ and $MoVTeNbBiO_x$ catalysts.

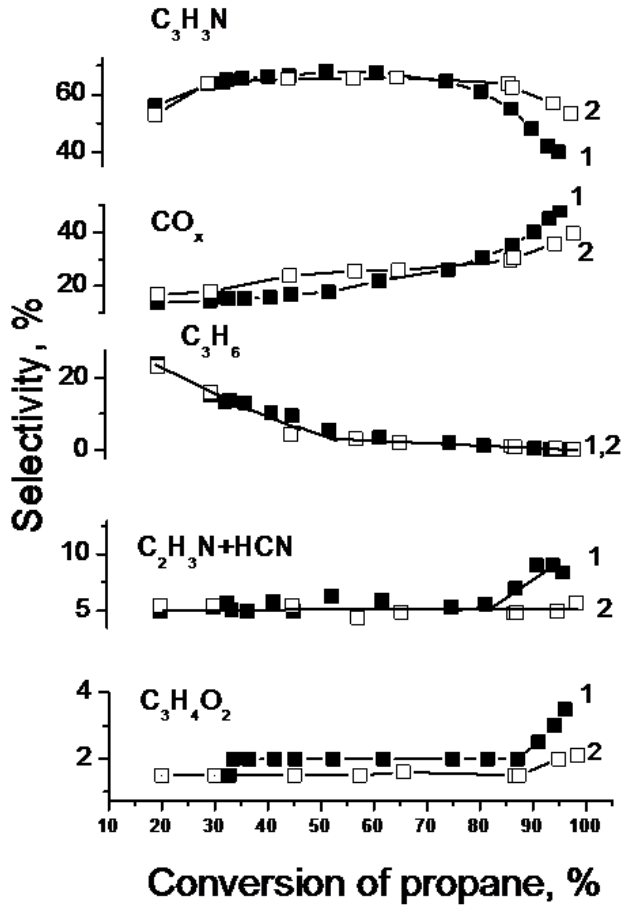

Fig. 2. The selectivity towards propylene (C_3H_6), acrylonitrile (C_3H_3N), CO_x, acrylic acid ($C_3H_4O_2$), acetonitrile and hydrocyanic acid (C_2H_3N+HCN) as a function of propane conversion on the $Mo_1V_{0.28}Te_{0.14}Nb_{0.13}O_x$ (curve 1) and $Mo_1V_{0.28}Te_{0.18}Nb_{0.11}Bi_{0.01}O_x$ (curve 2) catalysts.

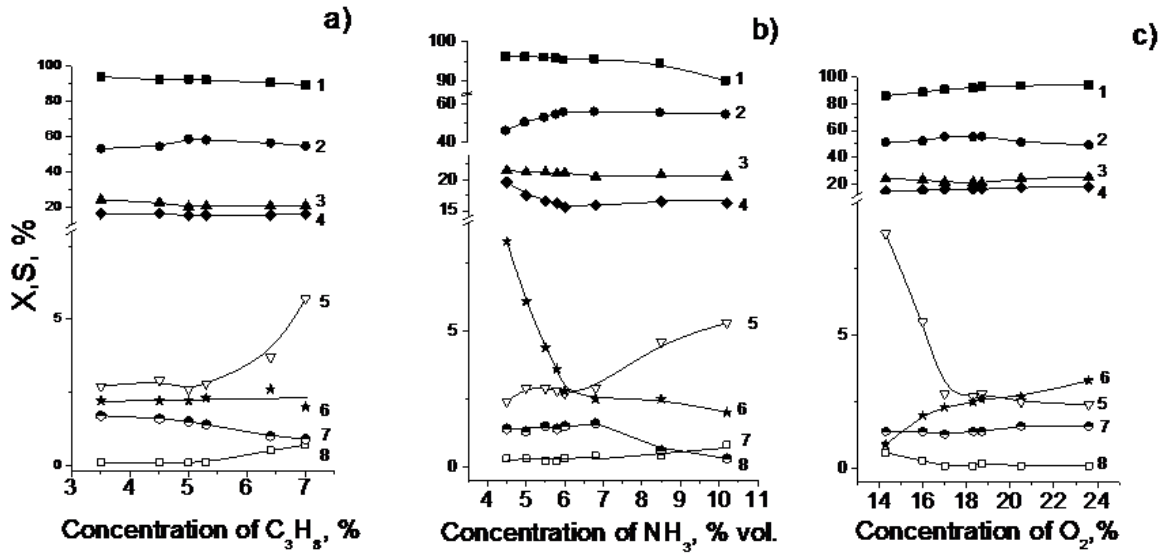

Fig. 3. Propane conversion (1) and selectivity towards reaction products (2-8) versus concentration of C_3H_6 (a); NH_3 (b) and O_2 (c). 2 - C_3H_3N, 3 - CO_2, 4 - CO, 5 - C_2H_3N, 6 - $C_3H_4O_2$, 7 - HCN, 8 - C_3H_6. $Mo_1V_{0.28}Te_{0.18}Nb_{0.11}Bi_{0.01}O_x$ catalyst was tested.

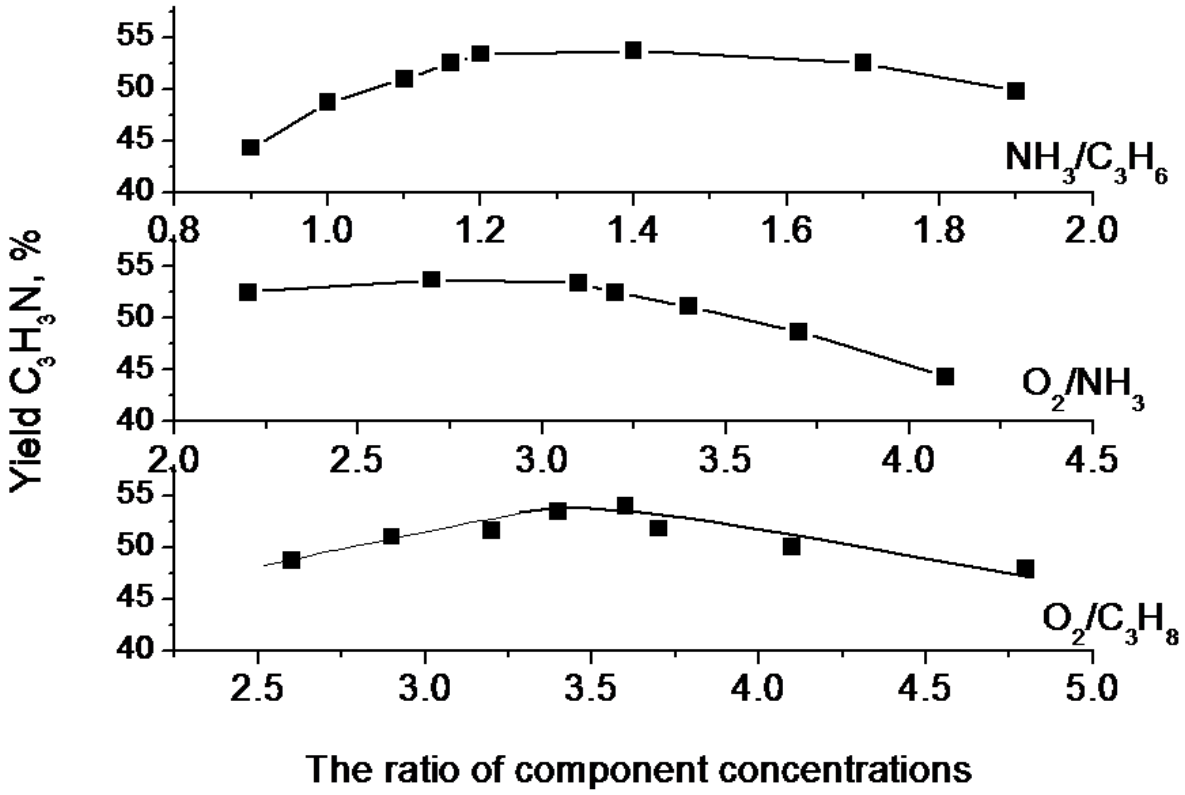

Fig. 4. Acrylonitrile yield versus the ratio of component concentrations. $Mo_1V_{0.28}Te_{0.18}Nb_{0.11}Bi_{0.01}O_x$ catalyst was tested.

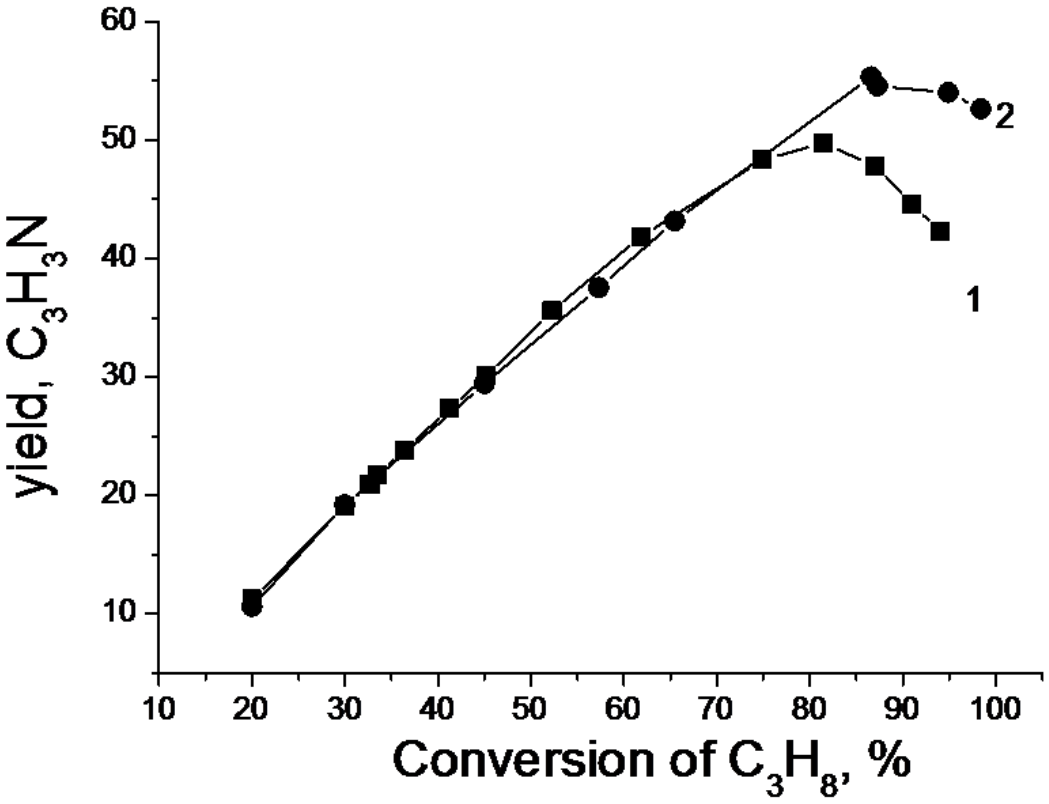

Fig. 5. Dependence of acrylonitrile yield on propane conversion at the reaction temperature 420 °C on the $Mo_1V_{0.28}Te_{0.14}Nb_{0.13}O_x$ (curve 1) and $Mo_1V_{0.28}Te_{0.18}Nb_{0.11}Bi_{0.01}O_x$ (curve 2) catalysts.

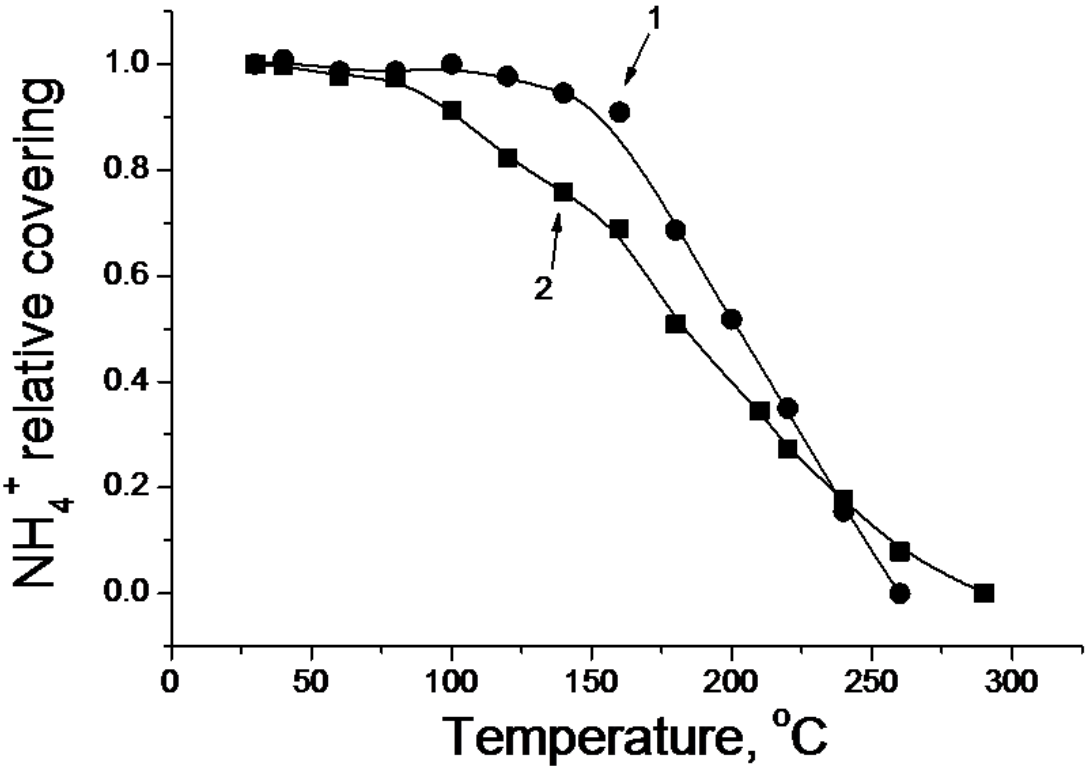

Fig. 6. Dependence of NH_4^+ relative covering upon temperature obtained in the TPD experiment on the $Mo_1V_{0.28}Te_{0.14}Nb_{0.13}O_x$ (curve 1) and $Mo_1V_{0.28}Te_{0.18}Nb_{0.11}Bi_{0.01}O_x$ (curve 2) catalysts.

Tables

Table 1. Physicochemical properties of the samples under study

Chemical composition of the catalysts		
before calcinations	after calcination	S_{BET}, m^2/g
$Mo_1V_{0.3}Te_{0.23}Nb_{0.12}$	$Mo_1V_{0.28}Te_{0.14}Nb_{0.13}$	7.3
$Mo_1V_{0.3}Te_{0.23}Nb_{0.12}Bi_{0.01}$	$Mo_1V_{0.28}Te_{0.18}Nb_{0.11}Bi_{0.01}$	7.0
$Mo_1V_{0.3}Te_{0.23}Nb_{0.12}Bi_{0.02}$	$Mo_1V_{0.3}Te_{0.17}Nb_{0.12}Bi_{0.02}$	6.1
$Mo_1V_{0.3}Te_{0.23}Nb_{0.12}Bi_{0.05}$	$Mo_1V_{0.28}Te_{0.23}Nb_{0.14}Bi_{0.05}$	5.0

Table 2. The $Mo3d_{5/2}$, $Te3d_{5/2}$, Nb3d, $V2p_{3/2}$, $Bi4f_{7/2}$ and O1s binding energies of the $Mo_1V_{0.28}Te_{0.14}Nb_{0.13}$ and $Mo_1V_{0.28}Te_{0.18}Nb_{0.11}Bi_{0.01}$ catalysts (eV).

Catalyst	$Mo3d_{5/2}$	$Te3d_{5/2}$	$Nb3d_{5/2}$	$V2p_{3/2}$	$Bi4f_{7/2}$	O1s
$Mo_1V_{0.28}Te_{0.14}Nb_{0.13}$	233.1	576.8	207.3	517.0	-	530.9
$Mo_1V_{0.28}Te_{0.18}Nb_{0.11}Bi_{0.01}$	233.2	577.0	207.4	517.2	159.9	531.0

Table 3. The results of XPS analysis. The M/Mo ratios according to XPS.

Catalyst	[Nb]/[Mo]	[Te]/[Mo]	[V]/[Mo]	[Bi]/[Mo]	[C]/[Mo]	[O]/[Mo]
$Mo_1V_{0.28}Te_{0.14}Nb_{0.13}$	0.13	0.25	0.15	-	1.4	3.4
$Mo_1V_{0.28}Te_{0.18}Nb_{0.11}Bi_{0.01}$	0.12	0.15	0.19	0.011	0.9	3.3

Table 4 Catalytic properties of MoVTeNb(Bi)O_x samples, C_3H_8/NH_3/air = 1/1.2/15, temperature 420 °C.

Bi/Mo	t, s	X,% C_3H_8	X, % NH_3	Selectivity, %					k, s^{-1}
				C_3H_3N	C_3H_6	C_2H_3N HCN	CO_x	$C_3H_4O_2$	
0	5.9	94.0	99.0	40.0	0.1	11.9	45.0	3.0	0.42
0.01	4.3	94.9	94.0	56.9	0.3	3.5	36.5	1.3	0.56
0.02	4.5	95.6	94.0	55.2	0.2	1.8	35.6	4.2	0.70
0.05	3.8	65.5	90.0	57.1	4.2	3.8	29.3	3.7	0.28
0.05	9.5	93.0	92.0	50.8	0.1	6.0	38.9	4.4	0.28

t - contact time; X – conversion, k - reaction rate constants.

The reaction rate constant values were calculated according to the first order integral equation describing the plug flow reactor: k= -ln(1-x)/t.